VOL. 12, NO. 15, AUGUST 2017 ISSN 1819-6608
ARPN Journal of Engineering and Applied Sciences

www.arpnjournals.com

ISLANDING DETECTION IN MICROGRID WITH WIND TURBINE AND REDUCE NON DETECTION ZONE

Abdolreza Behvandi, Mehrdad Kankanan and Omid Rahat
Department of Electrical Engineering, Ramhormoz Branch, Islamic Azad University, Ramhormoz, Iran
E-Mail: A-behvandi@phdstu.scu.ac.ir

ABSTRACT

The most important protective needs for connected microgrids to the network are detection and protection against islanding conditions. In this paper, a new method is presented for islanding detection condition for a standard microgrid equipped with various generation source including wind turbine with double feed induction generator(DFIG), CHP, photovoltaic. The proposed method for islanding detection conditions is based on injecting disturbed current through axis q or controller orthogonal axis of double feed induction generator- side converter. Therefore, by applying the proposed method, the variation frequency voltage of wind turbine stator is considered as islanding detection condition index. In this method, stator voltage is considered as islanding detection conditions signal is fed to a logical circuit, and then, the system frequency is studied and if the frequency exceeds the threshold (59.9-60.1) Hz, the conditions are detected as islanding conditions. The proposed method is able to detect islanding conditions in comparison to mentioned transient states that result in significant decrease in NDZ. The simulation result, using PSCAD/EMTDC, shows the effectiveness of applying of the proposed method in islanding conditions detection.

Keywords: microgrid, islanding detection, nondetection zone, wind turbine.

INTRODUCTION

Microgrid, designed as small low-voltage units to supply thermal and electrical local loads in suburbs, universities and industrial and commercial centers, are basically distributed active networks, because they connect distributed generators and different load in distribution voltage levels to each other [1].

The most important protective needs for connected microgrids to the network are detecting and protecting against islanding conditions. According to IEEE Std.1547.1, islanding conditions in distributed generators is an electrical phenomena , and it occurs when the utility grid injected power due to different reasons interrupted and distributed generators supply the load partially or completely[2,3]. Islanding conditions happen in two ways, planned and unwanted, because of natural incidents and human mistakes, that in unwanted islanding conditions several problems will occur for microgrid [5, 6].

That reliability of islanding detection methods and the efficiency of islanding prevention methods usually evaluated regarding nondetected zones conditions (NDZ). The nondetected zones refer to interval based on difference between supplied power by distributed generator inverter and consumed power by load that in these intervals, that inverter islanding detection method fails in correct detection of islanding condition [7-9].

Islanding detection methods are divided into local and remote methods. In remote methods, the operator monitors the islanding information network and control relays directly. Although methods have high reliability, costly implementation and complexity of applied techniques are the obstacles of the remote methods [8, 10-14]. Local methods use the available data and quantities in the output of distributed generation unit. The most important advantages of local method in comparison to remote methods, are low cost and ease of implementation [2, 11, 14, 15]. Local detection methods are divided into passive and active. The passive methods use the measured values in the network. The passive methods don't interfere with the operation of distributed sources and microgrid. The threshold is set for these measurements, and when these measured values exceed the threshold, the microgrid trip relays are triggered in the main network. Determining the valid limits is one of the challenging sections in this method [2, 8]. Voltage variation, frequency variation rate, and power variation rate, and frequency variation and measuring the impedance variation are examples of passive islanding detection methods [12, 16]. Active methods use signal injection, positive feedback and controlled disturbance in order to provide islanding detection index. Disturbance injection, of course, has little influence on network parameters in the normal operating conditions, but in the islanding conditions, these disturbances, cause the parameters to exceed the threshold and detected as islanding. Some active methods are method based on voltage variation and Reactive power export, voltage disturbance injection[14], active frequency difference, sandia frequency shift and slip-mode frequency shift [5, 12]. Slip-mode frequency shift detection methods(SMS), active frequency difference(AFD) and sandia frequency shift(SFS) use positive feedback in order to make the PV inverter unstable in absence of grid through. very easy implementation, less NDZ than passive methods, and balance between the efficiency of this method and the output power quality and transient conditions are the advantages of these methods.

For most references that have been presented for islanding detection, the proposed detection methods implemented on a simple network including an indefinite source, a distributed source, and on RLC load, and the validity of operation of these methods for real and bigger microgrids is not proved. The distributed source is usually modeled by an inverter model that this model is not the same for different distributed source such as DFIG, CHP,

and PV cells [3, 7, 8, 17]. In this paper, the proposed islanding conditions detection method for a standard microgrid equipped with various generating source including wind turbine with double feed induction generator (DFIG) and photovoltaic is presented. The operation of proposed method is based on the variation of the frequency of stator voltage of wind turbine. The islanding conditions detection method is an active method that is based on current disturbance injection through the wind turbine controller. In this method, the stator voltage is fed into a logical circuit as the islanding conditions detection signal. To study the capabilities of the proposed method, different operating conditions that result in islanding, transient states due to starting induction motors are studied. PSCAD/EMTDC is used to simulation the system under study. In second section, the controlling procedure of double feed induction generator will be explained briefly. In third section, the proposed method for islanding conditions detection, that is based on current injection through the converter controller of double feed induction generator side, is presented. In the rest of this section, variation in distributed sources controllers, especially wind turbine with double feed induction generator, will be explained. Also, in the fourth section, the simulation result of operation are presented.

Modeling and structure of the distributed generation source

Wind turbine with double feed induction generator consists of three parts: double feed induction generator, back-to-back converter and appropriate controllers. This section is allocated for generator modeling. In this process, it is tried that simplification is done in a way that by keeping the necessary accuracy from the network and generator prospective, the calculation speed increases and the capability of using the model along with other elements of enormous network will be available.

A. The double feed induction generator model

The model of DFIG is shown in Figure-1. The induction generator is modeled like a wound induction generator that the rotor winding voltage is not zero. So, the Park's transformation is used and the machine equations in two axes, d and q, are presented. In generator modeling, by neglecting the generator transient states and the variation of flux per second, the machine equations are as below [11, 18]:

$$V_{ds} = -R_s i_{ds} - \omega_s \psi_{qs} \quad (1)$$

$$V_{qs} = -R_s i_{qs} + \omega_s \psi_{ds} \quad (2)$$

$$V_{dr} = -R_r i_{dr} - s\omega_s \psi_{qr} \quad (3)$$

$$V_{qr} = -R_r i_{qr} + s\omega_s \psi_{dr} \quad (4)$$

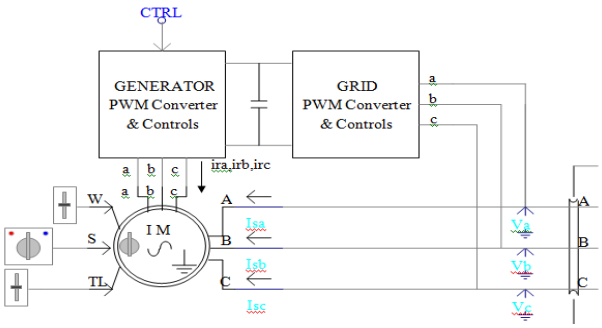

Figure-1. Model of double feed induction generator.

Where V is voltage of machine terminals in volts, R is winding resistance in Ohm, I is phase current in Apmers, ω_s is stator electrical frequency in rad/s, ψ is leakage flux of windings in weber and s is machine slip. The equations of leakage flux are completely mentioned in reference [21, 22].

B. Vector controlling of DFIG

As it is shown in Figure-1, vector controlling of DFIG consists of two major parts: converter controlling on network side (GSC), and converter controlling on rotor side (RSC).

a) GSC Controlling

On the one hand, the converter on network side is connected to the DC link. On the other hand, it is connected to the network. The goal of applying the converter on network side is to keep the voltage of DC link fixed. This is done by controlling d and q components. Figure-2 shows the diagram of converter controlling on network side.

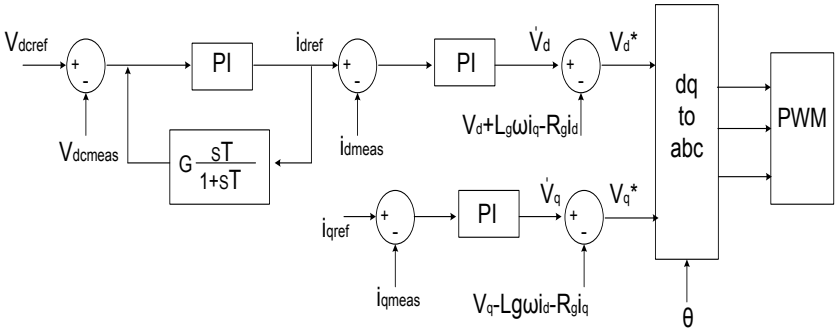

Figure-2. Diagram of converter controlling on network side.

V_{decref} In this controller, the measured voltage of dc link is subtracted from the reference voltage of DC link (V_{dcref}) and this value is fed into the PI controller and the converter output is considered as reference of d component. The difference between this current and the measured current (i_{dmeas}) is fed into current controller and the output of this controller is the auxiliary reference voltage (V_d'). The real voltage is gained through the following expression [23, 24]:

$$V_d^* = V_d + L_g\omega i_q - R_g i_d - V_d' \quad (5)$$

The index g is the transformer parameter after the converter on network side. q Component is set in the same direction of stator voltage. Thus, i_{qref} is set to zero. The difference between the current of q component and the measured current ($i_{qref} - i_{qmeas}$) is considered as the input of PI controller. The output of the controller is considered as auxiliary reference voltage (V_q'). The following expression is considered to gain the real voltage [23, 24]:

$$V_q^* = V_q + L_g\omega i_d - R_g i_q - V_q' \quad (6)$$

b) RSC Controlling

The controller on rotor side is used to control the output power into the network. The active and reactive power is considered as converter controller inputs on rotor side. Figure-3 shows the diagram of converter controller on rotor side.

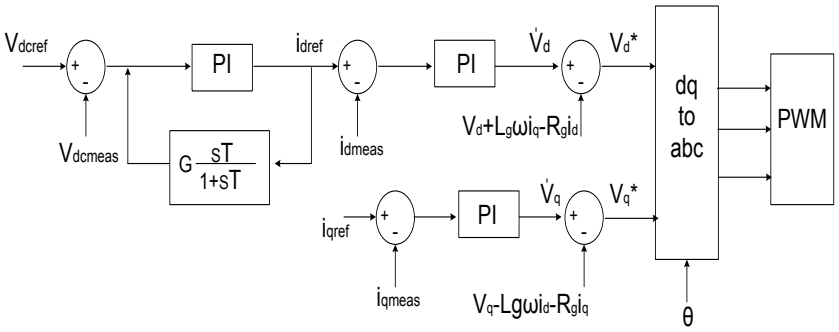

Figure-3. Diagram of converter controller on rotor side.

In order to set the q component, the inverter voltage is gained from current component by using active power. In order to gain the current component, first, torque is gained from active power, and then, the current is gained from torque. The following expressions show how current is gained from active power [24]:

$$T_e = \frac{P_m - P_{loss}}{\omega_r} \quad (7)$$

$$i_{dr} = \frac{T_e}{|\psi_s| . L_m / L_s} \quad (8)$$

In these relations, first, the mechanical torque is gained from (9), and then, the current of q component is gained from (10). The difference between the current of reference q component and the measured current ($i_{qref} - i_{qmeas}$) will be the PI controller input. The controller output is auxiliary reference voltage (V_q') that by applying it in the following expression, the q component voltage is made [21]:

$$V_q^* = R_r i_{qr} + L_r\omega i_{dr} + L_m\omega_r i_{ds} + \acute{V}_q \quad (9)$$

The reference current of d component is gained from instantaneous reactive power. There, the d component of inverter reference voltage is gained from the following equation [24]:

$$V_d^* = R_r i_{dr} - L_r\omega i_{qr} - L_m\omega_r i_{qs} + \acute{V}_d \quad (10)$$

In this equation, (V_d') is the auxiliary reference voltage that is gained from the output of current PI controller. The current of d component, also is the output of reactive power controller that its input is the difference between the reference reactive power and the measured reactive power ($Q_{ref} - Q_{meas}$). The model of photovoltaic structure and CHP, used in this paper, are shown in [3, 25] and [26, 27], respectively.

The proposed methods of islanding conditions detection

In this part, the proposed method to detect islanding conditions is presented. This detection method is based on active methods that according to them, by injecting disturbance and monitoring the desired index signals in the proposed method, the islanding conditions detection will be carried out. Later in this part, it will be shown that by using the islanding conditions detection method and by suitable change in wind turbine controller, the system stability can be kept in islanding conditions and prevented the black out of consumers. Also, microgrid is able to have a good operation in controlling the control frequency and voltage.

The structure of the proposed method of islanding conditions

The proposed method to detect islanding detection is injecting current through axis q. this current injecting methods is an active method. In this method, by injecting suitable disturbance and measuring frequency variation of wind turbine stator voltage as the islanding condition detection index, the islanding conditions will be detected.

In this method, the disturbance signal (i_{dist}) is injected to the utility gird with frequency different from the utility grid frequency (60Hz) and an amplitude equal to 0.1 of reference current of the stator d component. The disturbance signal is defined as below:

$$i_{dist} = i_d \cos(\omega_d t) = i_d \cos(2\pi f_d t) \quad (11)$$

This disturbance signal must injected to the utility grid through the controller on wind turbine with double feed induction generator (DFIG) side. Thus, the proposed method is based on the fact that the stator voltage of induction generator is fed into a zero-crossing detector, according to the Figure-4, as the islanding detection index. By comparing the output of zero-crossing detector with zero, while crossing from the positive cycle to the negative cycle, the output of zero-crossing detection system is set to 1. It must be notified that the zero-crossing from positive cycle to negative cycle is not calculated. The output of this comparator is fed into a monostable with T_1= 16.693 ms that is corresponding to 60.1 Hz. The output of this monostable is reversed and is fed into another monostable with T_2= 55.6 ms that is corresponding to Δf= 0.2 Hz. The output of second monostable consists the control signal. The values of T_1 and T_2 are set to detect the deviation when the frequency exceeds the range 60.1-59.9 Hz.

The reference and control signals are controlled by the logical circuit in Figure-4 when the reference signal of detection circuit detects the zero-crossing from negative to positive cycle; the control signal is set to 1. If the control s signal is 1, that is, the frequency is in range 60.1-59.9 Hz. Therefore, if the reference signal is 1 and the control signal is zero, that is, frequency is out of its threshold, and thus, by feeding the output of both control and reference signal logical circuit into a monostable, by an acceptable delay, the islanding conditions can be distinguished from other conditions such as induction motor starting and load switching.

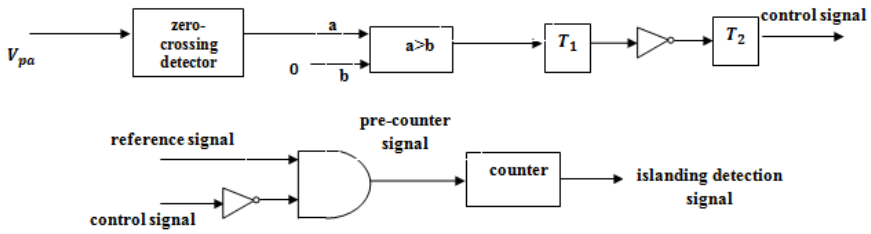

Figure-4. Diagram of proposed methods of islanding conditions detection.

The operation of microgrid in islanding conditions

In islanding operation, in order to minimize the dynamic of system and damping of output power transient fluctuations in a place that no infinite network is available, the In islanding operation, in order to minimize the dynamic of system and damping of output power transient fluctuations in a place that no infinite network is available, the flexible and fast active/reactive power control strategy is necessary [27]. In these conditions, the CHP source that is equipped with governor and excitation systems, by using the voltage excitation system is set to 1 pu. Also, by using the governor system that is based on frequency-active power equation, it controls the disturbance in generator speed. In addition, the wind turbine with double feed induction generator, changes to islanding state by applying primary control frequency and setting the output voltage of rotor-dq axis current.

Primary frequency control

One of the wind turbine characteristics is variable speed that in spite of the design of the thermal and gas turbine, they can increase their power instantaneously [26]. This is an important feature, especially, for the microgrid systems when they change to the islanding operation.

The primary frequency control shown in Figure-5 is added to active power control loop in converter on rotor side shown in Figure-3. This frequency control is similar to frequency-power control loop that is usually used in synchronous generator. Thus, increase in active power is corresponding of variation in system frequency that is defined as below:

$$P_{injected} = P_{ref} - (\frac{1}{R})(\omega_{sys} - \omega_{ref}) \quad (12)$$

$P_{injected}$, P_{ref}, R, ω_{sys} and ω_{ref} are injected power by double feed induction generator, the reference power of double feed induction generator, drop, the angular velocity of double feed induction generator and reference angular velocity, respectively.

This generated active power needs the new operating point of DFIG. So, primary frequency control is exerted on the active power controller in converter on rotor side. It must be noticed that this feature (primary frequency controller) is exerted only under islanding state operation. ω_{sys} is gained from DFIG busbar connected to the network using the phase look loop (PLL). The active power controller is shown in Figure-5.

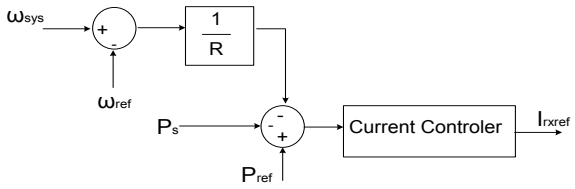

Figure-5. The primary frequency control.

Reactive power control and the output voltage regulation

Speed variant wind turbine with DFIG has the capability of regulating its own voltage. This is considered an important feature for operation in islanding state. With this feature, the wind turbine can participate in reactive power management and regulate the microgrid voltage. In connected to the network operation, while ignoring the resistance of induction generator stator, the reactive power is exerted directly like Figure-3. it can be shown that the relation between the generated reactive power and the current of rotor d component (i_{rxref}) is mentioned below[23]:

$$Q_s = -(\frac{L_m}{L_{ss}})(i_{rxref} + i_{dr,gen}) - \frac{{V_{sq}}^2}{\omega_s(L_{ss})} \quad (13)$$

$Q_s, L_s, V_{sq}, \omega_s$ show stator reactive power, stator inductance, the mutual stator inductance, the voltage of q axis, and nominal angular velocity, respectively. i_{rxref}, as rotor d component current, determines the magnetizing reactive power of induction generator and also, $i_{dr,gen}$, determines the exchange power between utility grid and induction generator.

In connected-to-the-network conditions, by applyingi_{rxref}, the reactive power of DFIG is determined [23]. For operation in islanding conditions and the voltage regulation, one control loop is added to current control of i_{rxref} component as Figure-6 by using this control loop, the reactive power of wind turbine is managed.

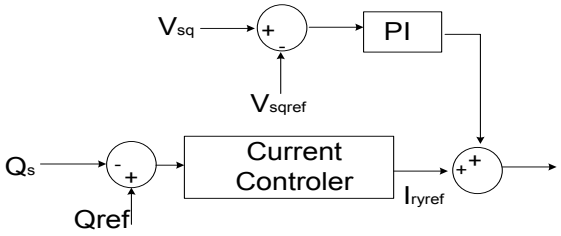

Figure-6. The terminal voltage controller of DFIG in islanding condition.

THE RESULT OF THE PROPOSED METHOD SIMULATION

In this section, the proposed method for detecting islanding conditions of the studied system in Figure-7 is simulated and operation under different circumstances will be evaluated.

A. Introducing the system under study

In Figure-7, the structure of a medium voltage distribution network with several distributed generation sources is shown that is introduced as the test network for studying the connection of distributed source by the International Council on Large Electric Systems (CIGRE) [28]. The nominal voltage of the network is 20 kV that is fed by the 110 kV transfer substation. By occurring a fault in the system and opening the main switch (that lies in the secondary of transformer TR1), microgrid continues its operation separately or so-called islanding condition. Also, there are two switch close to busbars 4 and 7 that are normally open and by closing them, the distribution system with ring structure can be investigated.

The standard microgrid structure, studied in this paper, has 3 distribution generation units of wind turbine with DFIG, photovoltaic and CHP. The transmission line parameters and loads of standard network, wind turbine with induction generator, the photovoltaic generation system, and CHP are listed in the appendix.

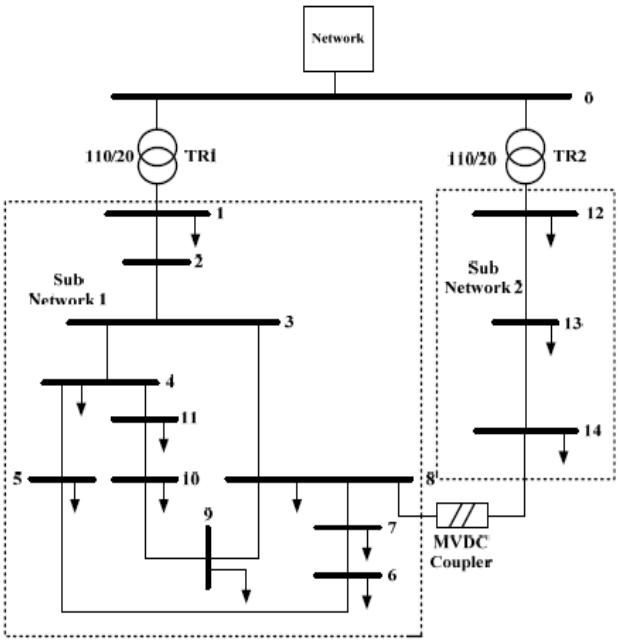

Figure-7. System under study [28].

B. The Simulation Results

In this section, the simulation results of normal conditions operation of system, the operation of islanding conditions detection method, the operation of detection method under the condition of starting of induction motor will be studied.

a) The normal operation of system

In this section, the normal operating conditions of system under study, in order to better understanding of islanding conditions detection, will be shown. Figure-8 shows the stator voltage of DFIG in pu. As it can be seen, the voltage value is 1 pu.

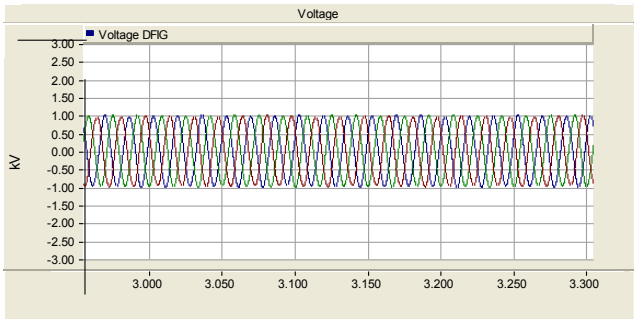

Figure-8. Stator voltage of DFIG in the normal operating.

The amount of active load in microgrid is P_{load} =2.821 MW. Thus, in these conditions, the amount of supplied active power from utility grid, DFIG, CHP and photovoltaic will be P_{grid} =0.55 MW, P_{DFIG} =0.9 MW, P_{CHP} =1.2 MW, P_{pv} =0.25 MW, respectively.

The amount of reactive power of wind turbine with DFIG is shown in Figure-9 as well. The amount of reactive load in microgrid is Q_{load} =1.148 MVar. In these conditions, the amount of supplied reactive power by utility grid and microgrid generating units are Q_{grid} =1.6 MVar, $Q_{DFIG} = -0.5$ MVar, $Q_{CHP} = -0.8$ MVar, Q_{pv} =0.15 MVar, respectively.

Figure-9 also shows the frequency of DFIG bus in normal operating conditions of system. As it can be seen, the desired DFIG frequency, with some fluctuation, lies in valid range of (60.1-59.9) Hz.

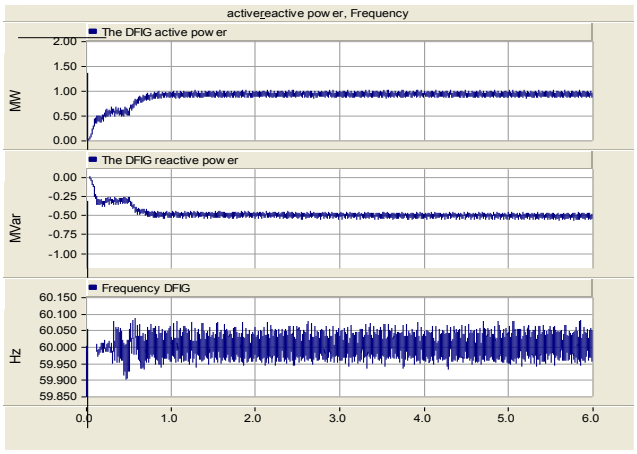

Figure-9. Active power, reactive power and frequency of DFIG in the normal operating.

b) The system operation under islanding conditions

In this section, the instant that microgrid connection to utility grid is lost, whether planned or unwanted, and the microgrid operation under islanding conditions will be studied and simulated.

In this simulation, to detect islanding conditions, it is assumed that, planned or unwanted, the main switch (that connects the main network to the microgrid) will be open in t=3 sec. afterwards, the microgrid is separated from utility grid, thus, it lies in islanding operation conditions. The voltage and frequency control is done by utility grid while the microgrid is connected to the utility grid. In islanding conditions, the utility grid will lose its control on voltage and frequency. Therefore, in islanding conditions, in order to control the voltage and frequency, change in microgrid controllers will be necessary.

Figure-10 shows the stator voltage of DFIG in pu. In t=3 sec, the utility gird has no control on microgrid voltage due to islanding conditions, thus, the stator values of DFIG bus are exposed to disturbance. So, the change in microgrid controllers is inevitable. The changes cause, after about 100 ms of occurring islanding conditions, the stator voltage value of DFIG bus to be set in 1 pu.

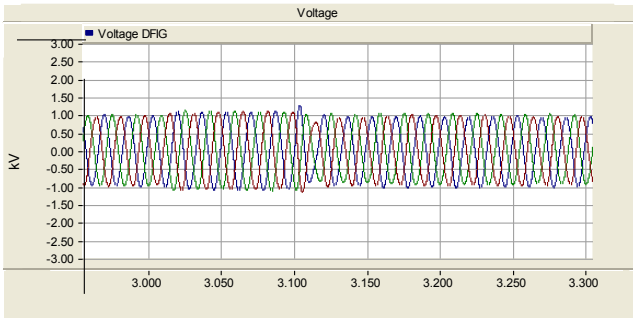

Figure-10. The stator voltage of DFIG in the instant that microgrid connection to utility grid is lost and operation under islanding conditions.

Figure-11 shows the active power of DFIG, before and after islanding conditions. In conditions after islanding, the utility grid power will be zero, and the active of microgrid generating units won't change noticeably. As a result, failure in supplying the microgrid load by these sources causes fluctuations in microgrid frequency. Thus, by changing microgrid controllers, both the DFIG and CHP active power will increase by 0.3 MW. The photovoltaic power that supplies small amount of active power won't change dramatically because of working at its maximum generation.

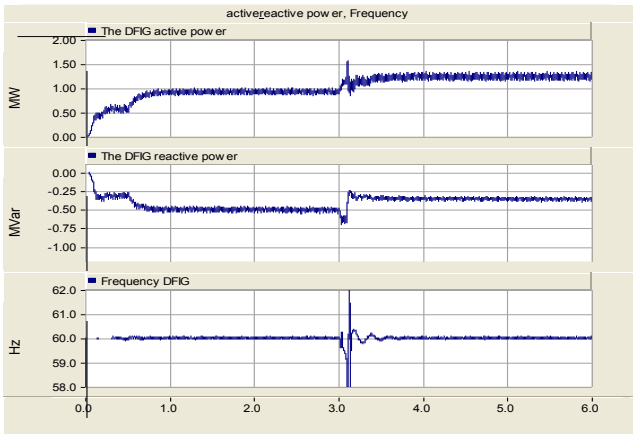

Figure-11. Active power, reactive power and frequency of DFIG in the instant that microgrid connection to utility grid is lost and operation under islanding conditions.

Also, in Figure-11, the DFIG reactive power is shown. In islanding conditions operation, the reactive power of utility grid is zero, and the reactive powers of DFIG and CHP are $Q_{DFIG} = -0.36$ MVar and $Q_{CHP} = -0.5$ MVar, respectively. The required microgrid reactive power is compensated by compensator capacitor in DFIG busbar and change in microgrid controller.

At the moment of islanding occurrence, the DFIG busbar frequency fluctuates. So, when the frequency exceeds the threshold (59.9-60.1) Hz, the proposed method detects this frequency fluctuation. The fluctuation of DFIG busbar is shown in Figure-12. As it can be seen, frequency lies in the valid range at t=3.1 sec.

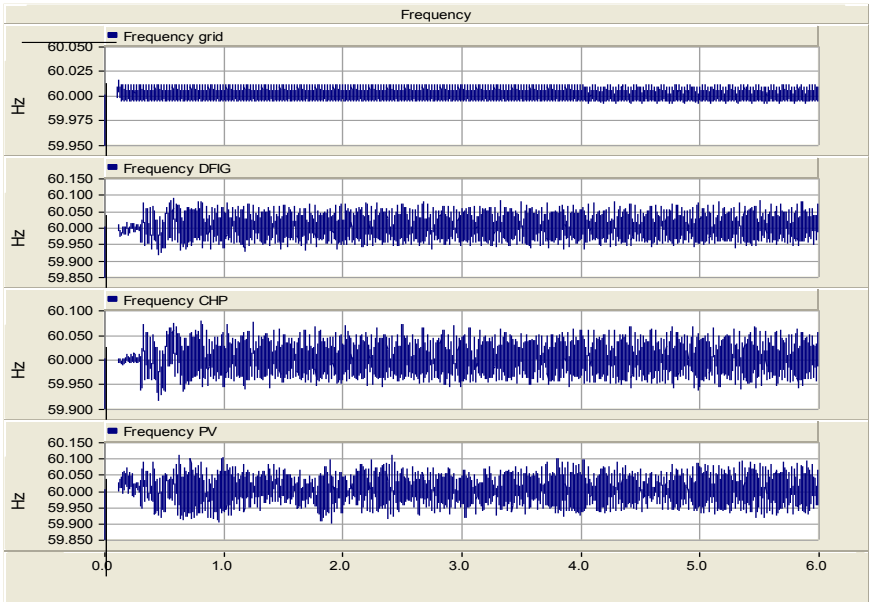

Figure-12. Frequency of utility grid, DFIG busbar, CHP busbar and PV busbar.

The stator voltage of DFIG is considered as the index of islanding conditions detection based on proposed method explained in section 3. According to Figure-13, when the microgrid is disconnected from the utility grid, the power swing causes the frequency of DFIG voltage exceeds the valid range and, thus, the islanding conditions detection system detects the islanding conditions in 65 ms after the disconnection of microgrid from utility grid. According to this detection and 100 ms after islanding conditions, frequency fluctuations lie in valid range (59.9-60.1) Hz that this is because of change in microgrid controllers for frequency control.

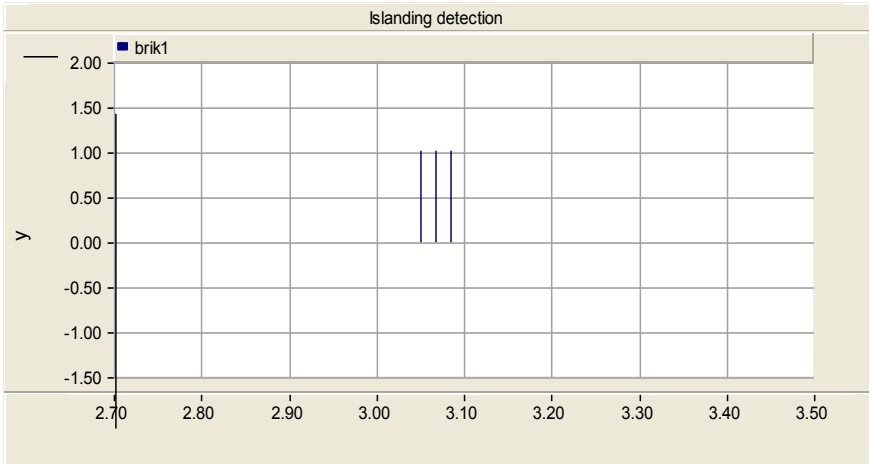

Figure-13. Signal of islanding detections in the instant that microgrid connection to utility grid and operation under islanding conditions.

C. The System operation in induction motor starting conditions

The connection between microgrid and utility is not disconnected while some conditions occur in microgrid, and thus, the microgrid doesn't lie in islanding conditions.

In this paper, four induction motors with S= 0.475 MVA and $V_{L-L} = 0.4$ kV for each one are connected to the

microgrid busbar 3 through four transformers. This induction motor start operating at t= 3 sec. At this moment, as it is shown in Figure-14, the voltage of busbar 3 that the induction motor is connected to it through transformer, is imposed to a transient disturbance and after about 60 ms returns to its normal operation.

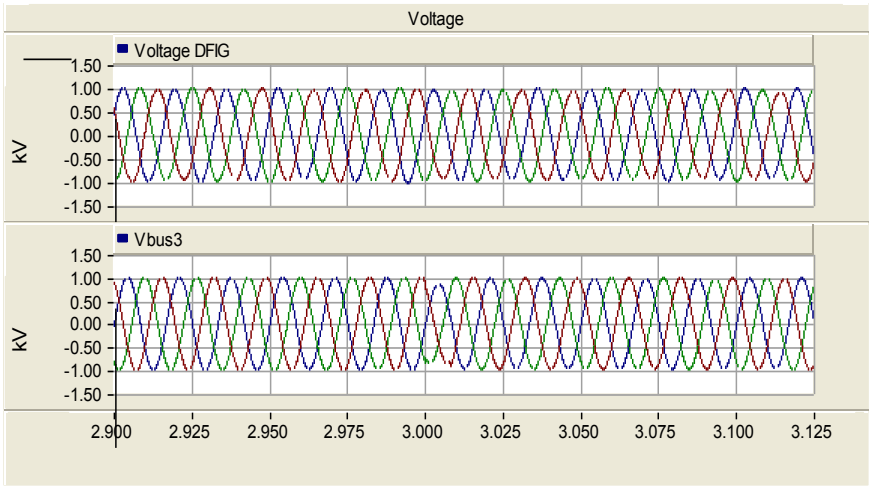

Figure-14. Stator voltage of DFIG and induction motor in induction motor starting conditions connected to the microgrid busbar 3.

The induction motor active power and reactive power are shown in Figure-15 under these conditions, its power will be P_{IM}= 1.27 MW and Q_{IM}= 1.2 Mvar after starting the induction motor. These amounts of consuming active and reactive power of induction motor will be provided by utility grid (that is considered as slack bus). thus, according to Figure-15, the network active and reactive power after induction motor starting increase as much as consuming active and reactive power, but the active and reactive power of microgrid generating source will stay in their normal operating value.

According to Figures-16 and Figure-17, despite the presence of motor starting and transient frequency fluctuation, the proposed method has desired operation and doesn't detect these conditions as islanding conditions.

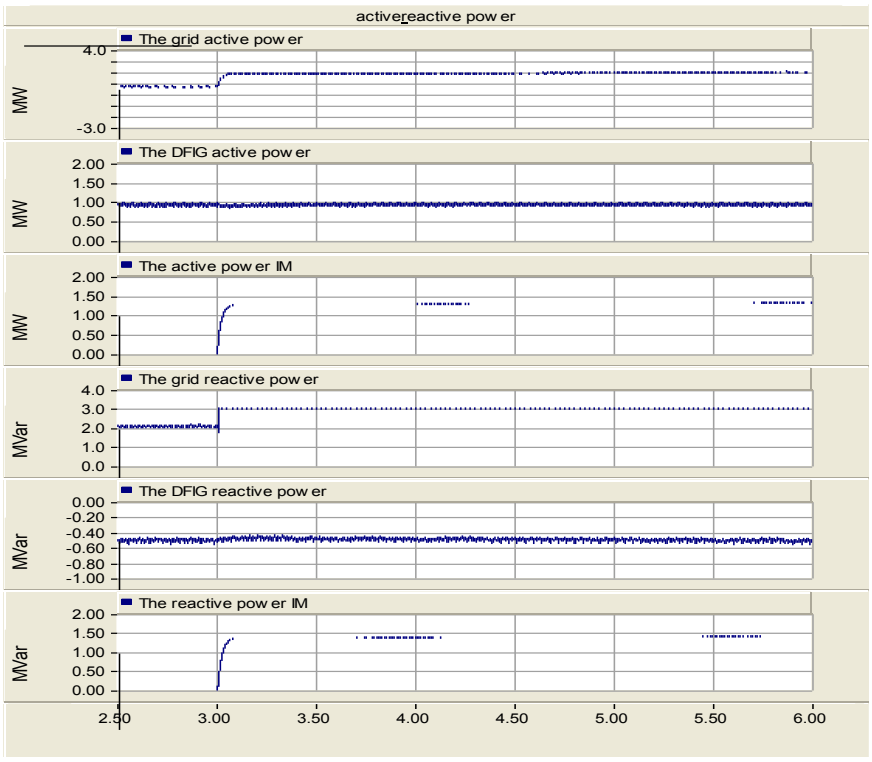

Figure-15. Active power and reactive power of utility grid, DFIG and induction motor in induction motor starting conditions connected to the microgrid busbar 3.

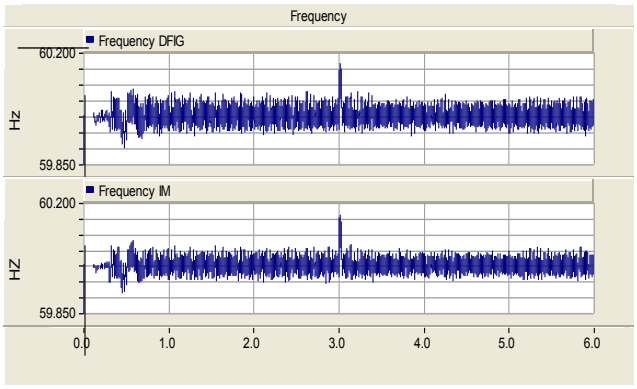

Figure-16. DFIG frequency and induction motor in induction motor starting conditions connected to the microgrid busbar 3.

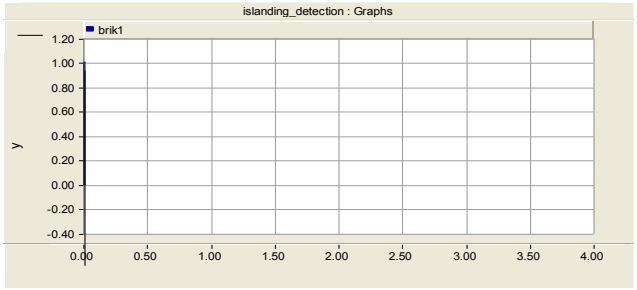

Figure-17. Signal of islanding detections in induction motor starting conditions connected to the microgrid busbar 3.

CONCLUSIONS

In this paper, the proposed method to detect islanding conditions in a standard microgrid is simulated. This standard microgrid consists of generating sources including wind turbine with DFIG, CHP, and photovoltaic generating system (PV). The propose method to detect islanding conditions is an active method that is based on disturbance current injection through the converter controller on wind turbine with DFIG side, the islanding conditions are detected. In this proposed method the variant of frequency of induction generator stator voltage is considered as the islanding conditions detection index. In this paper, the dynamic modeling of generating source and their controlling system, and microgrid operation is studied and simulated close to real conditions.

To make the microgrid be able to continue its desirable operation in islanding conditions and provided the microgrid loads. it is necessary to change the available controllers in microgrid. The simulated results prove that in islanding conditions by applying the proposed variations, the microgrid has desirable operation and by power generation distribution among generating source, the load in microgrid will be supplied. In a few conditions that happen in the microgrid, the connection between microgrid and utility grid is not lost, thus, the microgrid won't lie in islanding conditions. Because of this, one of important criteria to prove the proper operation of islanding conditions detection is the distinct that exists between these conditions and islanding conditions. In this paper, the induction motor starting and one of the microgrid lines disconnections are studied as two distinctive conditions of islanding conditions. The desirable operation of the proposed method is proved by the distinction between these conditions and islanding conditions regarding simulation results.

ACKNOWLEDGEMENT

Funding support of this research was provided by the Ramhormoz branch, Islamic Azad University, Ramhormoz, Iran. Moreover this paper was derived from a report named "Islanding Detection in Microgrid with Wind Turbine and Reduce Non Detection Zone".

APPENDIX

A. DFIG

Parameter	Value	Parameter	Value
R_r	0.00607 pu	$V_{L-L,rms}$	0.4 kV
L_{lr}	0.11 pu	S	1.5 MVA
L_{lm}	4.362 pu	R_s	0.0054 pu
H	0.363 s	$\boldsymbol{L_{ls}}$	0.102 pu

B. PV

Parameter	Value	Parameter	Value
C_f	2500 µF	V_{dc}	0.4 kV
R_f	1.5 Ω	L_f	0.0015 H
f_c	1800 Hz		

C. CHP

Parameter	Value	Parameter	Value
$T_{do}^{"}$	0.039 s	$T_{do}^{'}$	6.55 s
X_d	0.99117 pu	$\acute{X_d}$	0.18426 pu
X_q	0.68 pu	$\acute{X_q}$	0.224 pu
$X_d^{"}$	0.108 pu	$X_q^{"}$	0.108 pu
$V_{L-L,rms}$	13.8 kV	R_a	0.0052 pu
$T_{qo}^{"}$	0.071 s	$T_{qo}^{"}$	0.071 s
H			

D. Induction Motor

Parameter	Value	Parameter	Value
L_{ls}	0.0613 pu	R_s	1 pu
$V_{L-L,rms}$	0.4 kV	S	0.475 MVA
H	0.15 s	L_{lm}	1 pu
L_{lr}	0.0613 pu	R_r	0.1 pu

REFERENCES

[1] S. Chowdhury, S.P. Chowdhury, P. Crossley. 2009. Microgrids and Active Distribution Networks. The Institution of Engineering and Technology, ISBN 978-1-84919-014-5.

[2] J.C Ho., K.J. Chua and S.K. Chou. 2004. Performance Study of a Microturbine System for Cogeneration Application. Renewable Energy. 29(7): 1121-1133.

[3] H. Karimi, A. Yazdani, R. Iravani. 2008. Negative-Sequence Current Injection for Fast Islanding Detection of a Distributed Resource Unit. IEEE Transaction on Power Electronics. 23(1): 298-307.

[4] Jun Zhang, Dehong Xu, Guoqiao Shen, Ye Zhu, Ning He, and Jie Ma. 2013. An Improved Islanding Detection Method for a Grid-Connected Inverter with Intermittent Bilateral Reactive Power Variation. IEEE Transactions on Power Electronics. 28(1): 268-278.

[5] 2005. System operation with high wind penetration. IEEE power & energy magazine.

[6] H. Vahedi, R. Noroozian, A. Jalilvand, G.B. Gharehpetian. 2011. A New Method for Islanding Detection of Inverter-Based Distributed Generation Using DC-Link Voltage Control. IEEE Transaction Power on Delivery. 26(2): 1176-1186.

[7] W. Chiang, H. Jou, J. Wu, K. Wu, Y. Feng. 2010. Active Islanding Detection Method for The Grid-connected Photovoltaic Generation System. Electric Power Systems Research. 80(4): 372-379.

[8] B. Bahrani, H.Karimi, R. Iravani. 2011. Nondetection Zone Assessment of an Active Islanding Detection Method andits Experimental Evaluation. IEEE Transactions on Power Delivery. 26(2): 217-225.

[9] H. H. Zeineldin, M.M.A. Salama. 2011. Impact of Load Frequency Dependence on the NDZ and Performance of the SFS Islanding Detection Method. IEEE Transactions on Industrial Electronics. 58(1): 139-146.

[10] Mohamed Al Hosani, Member, IEEE, Zhihua Qu, Fellow, IEEE and H. H. Zeineldin, Senior Member. 2015. IEEE Scheduled Perturbation to Reduce Nondetection Zone for Low Gain Sandia Frequency Shift Method. IEEE Transactions on Smart Grid. 6(6): 3095-3103.

[11] D. Velasco, C. Trujillo, G. Garcer´a, E. Figueres. 2011. An Active Anti-Islanding Method Based on Phase-PLL Perturbation. IEEE Transaction on Power Electronics. 26(4): 1056-1066.

[12] D. Velasco, C.L. Trujillo, G. Garcera, E. Figueres. 2010. Review of Anti-islanding Techniques in Distributed Generators. Renewable and Sustainable Energy Reviews. 14(6): 1608-1614.

[13] P. Mahat, C. Zhe, B. Bak-Jensen. 2008. Review of Islanding Detection Methods for Distributed Generation. In: Third international conference on electric utility deregulation and restructuring and power technologies. pp. 2743-2748.

[14] A.M. Massoud, K.H. Ahmed, S.J. Finney, B.W. Williams. 2009. Harmonic Distortion Based Island Detection Technique for Inverter-based Distributed Generation. IETRenew. Power Gener. 3(4): 493-507.

[15] H. H. Zeineldin, J. L. Kirtley, Jr. 2009. A Simple Technique for Islanding Detection with Negligible Nondetection Zone. IEEE Transactions on Power Delivery. 24(2): 779-786.

[16] E.J. Estébanez, V.M. Moreno, A.Pigazo, M.Liserre, and A.D. Aquila. 2011. Performance Evaluation of Active Islanding-Detection Algorithms in Distributed-Generation Photovoltaic Systems: Two Inverters Case. IEEE Transactions on Industrial Electronics. 58(4): 1185-1193.

[17] Guillermo Hernández-Gonzálezand Reza Iravani. 2006. Current Injection for Active Islanding Detection of Electronically-Interfaced Distributed Resources" IEEE Trans. Power Delivery. 21(3); 1698-1705.

[18] Luiz A. C. Lopes, Yongzheng Zhang. 2008. Islanding Detection Assessment of Multi Inverter Systems with Active Frequency Drifting Methods. IEEE Trans. Power Deliv. 23(1): 480-186.

[19] Seul-Ki Kim, Jin-Hong, Heung-Kwan Choi, Jong-Yul Kim. 2011. Voltage Shift Acceleration Control for Anti-Islanding of Distributed Generation Inverters. IEEE Trans. Power Delivery. 26(4): 2223-2234.

[20] B. Bahrani, H. Karimi, R. Iravani. 2011. Nondetection Zone Assessment of an Active Islanding Detection Method and its Experimental Evaluation. IEEE Transaction on Power Delivery. 26(2): 517-525.

[21] Yazhou Lei, Alan Mullane, Gordon Lightbody and Robert Yacamini. 2006. Modeling of the Wind turbine with a doubly fed induction Generator for grid integration studies. IEEE transactions on energy conversion. 21(1).

[22] N. Senthil Kumar, J. Gokulakrishnan. 2011. Impact of FACTS controllers on the stability of power systems connected with doubly fed induction generators. Electrical Power and Energy Systems 33, pp. 1172-1184.

[23] P. Vas. 1998. Sensorless Vector and Direct Torque Control. Oxford University Press.

[24] H. Karimi, A. Sheikholeslami, H. Livani, N. Norouzi. 2008. Fault Ride through Capability Improvement of Wind Farms using Doubly Fed Induction Generation. UPEC 2008 43rd International Conference Universities Power engineering. pp. 1-5.

[25] R. Teodorescu, M. Liserre, P. Rodr´ıguez. 2011. Grid Converters for Photovoltaic and Power Systems. 2011 John Wiley & Sons, Ltd. ISBN: 978-0-470-05751-3.

[26] H. Geng, D. Xu, B. Wu, G. Yang. 2011. Active Islanding Detection foInverter-Based Distributed Generation Systems with Power Control Interface. IEEE Transaction on Energy Conversion. 26(4): 1063-1072.

[27] H. Knudsen and J. N. Nielsen. 2005. Introduction to the modeling of wind turbines. in Wind Power in Power Systems, T. Ackerman, Ed. Chicester, U.K.: Wiley. pp. 525-585.

[28] K. Rudion, A. Orths, Z. A. Styczynski, K. Strunz. 2006. Design of Benchmar of Medium Voltage Distribution Network for Investigation of DG Integration. IEEE.